Domain Engineering of Lead-Free Li-Modified (K, Na)NbO3 Polycrystals With Highly Enhanced Piezoelectricity

ARTICLE *in* ADVANCED FUNCTIONAL MATERIALS · JUNE 2010

Impact Factor: 11.81 · DOI: 10.1002/adfm.201000284

2 AUTHORS:

Ke Wang
Tsinghua University
60 PUBLICATIONS **1,589** CITATIONS
SEE PROFILE

Jingfeng Li
Tsinghua University
340 PUBLICATIONS **6,338** CITATIONS
SEE PROFILE

ADVANCED FUNCTIONAL MATERIALS
www.afm-journal.de

Materials Views
www.MaterialsViews.com

Domain Engineering of Lead-Free Li-Modified (K,Na)NbO_3 Polycrystals with Highly Enhanced Piezoelectricity

By *Ke Wang* and *Jing-Feng Li**

Aging and re-poling induced enhancement of piezoelectricity are found in (K,Na)NbO_3 (KNN)-based lead-free piezoelectric ceramics. For a compositionally optimized Li-doped composition, its piezoelectric coefficient d_{33} can be increased up to 324 pC N^{-1} even from a considerably high value (190 pC N^{-1}) by means of a re-poling treatment after room-temperature aging. Such a high d_{33} value is only reachable in KNN ceramics with complicated modifications using Ta and Sb dopants. High-angle X-ray diffraction analysis reveals apparent changes in the crystallographic orientations related to a 90° domain switching before and after the aging and re-poling process. A possible mechanism considering both defect migration and rotation of spontaneous polarization explains the experimental results. The present study provides a general approach towards piezoelectric response enhancement in KNN-based piezoelectric ceramics.

1. Introduction

Although piezoelectric materials have been in commercial use for a long time, further development of them has not ceased. One of the most concerning subjects is the search for lead-free counterparts to substitute the widely used lead zirconate titanate (PZT) ceramics, which are not environmentally friendly.[1,2] The breakthrough made by Saito et al.[3] in textured (Na,K)NbO_3 (KNN) ceramics with codopants of Li, Ta, and Sb has had a significant impact on the development of lead-free piezoelectric ceramics. In recent years, tremendous studies have been devoted to KNN-based ceramics with the emphasis on property enhancement by optimizing sintering processes and compositional modifications.[4,5] Previous studies have confirmed that Li doping of KNN is very effective and indispensable in enhancing its piezoelectric responses as well as its Curie temperature (T_C).[6–10] Although Ta and Sb can provide further improvement on the dielectric constant and piezoelectric coefficient,[7,11] their use is not favored because of the high cost of Ta and the toxicity of Sb. Therefore, simple Li-doped KNN is still a good candidate for use in lead-free piezoelectric ceramics.

[*] Prof. J.-F. Li, K. Wang
State Key Laboratory of New Ceramics and Fine Processing
Department of Materials Science and Engineering
Tsinghua University
Beijing 100084 (P.R. China)
E-mail: jingfeng@mail.tsinghua.edu.cn

DOI: 10.1002/adfm.201000284

Recently, a few studies have revealed that there are many possibilities to further enhance the piezoelectric properties of KNN-based ceramics even through simple Li-doping,[12] without additional compositional modifications by Ta and Sb. For example, our recent study demonstrated that a high piezoelectric coefficient d_{33} of up to 280 pC N^{-1} could be obtained in Li-doped KNN ceramics by elaborate adjusting of the Li content and Na/K ratio,[13] whereas the d_{33} of pure KNN ceramics is around 100 pC N^{-1}. Even for a fixed nominal composition, it was also possible to increase the piezoelectric constant d_{33} from about 220 pC N^{-1} to 314 pC N^{-1} in KNN-based ceramics doped only with $LiNbO_3$ by optimizing the sintering temperature.[14]

However, practical implementations of KNN-based ceramics, including those modified by multiple dopants of Li, Ta, and Sb, for commercial use are still limited by their inferior electrical and electromechanical properties as compared to their conventional PZT counterparts. Almost all the recent efforts contributing to property enhancement in KNN-based ceramics have been concentrated on chemical optimization, such as adjusting the proportions of the different kinds of dopants, in addition to control over the sintering process, which also changed the compositions slightly by means of volatilization of the alkali elements. In general, most reports have confirmed that the highest piezoelectric coefficient d_{33} that can be achieved in non-textured KNN-based ceramics is restricted to the region between 200 and 300 pC N^{-1}. The commonly mentioned piezoelectric coefficient, d_{33}, used here is the one that most people are concerned with, which is determined by the electric charge response to an external mechanical stress using a quasi-state d_{33} meter. It should be emphasized that the d_{33} coefficient is dominated by the intrinsic (lattice) piezoelectric responses, since extrinsic contributions mainly originate from non-180° domain wall motions and are negligible because of the small applied mechanical field.[15] For piezoceramics with a given composition, the improvement of d_{33} can only be accomplished by an increase of the relative permittivity ε_{33} or remnant polarization P_r, according to

$$d_{33} = 2Q_{11}\varepsilon_0\varepsilon_{33}P_3 \quad (1)$$

where P_3 is the polarization along the polar axis and approximately equals P_r in this case; Q_{11} is the electrostrictive

constant of the paraelectric phase and typically varies between 0.05 and 0.1 m^4 C^{-2} for different materials.[16] Improvement of the permittivity ε_{33} has been reported in other piezoceramics, such as $BaTiO_3$, by decreasing the grain size to an appropriate magnitude of around 0.7 μm;[17] however, microstructure adjustment in KNN-based ceramics is not so facile since densification of the ceramics itself is a big issue, which requires special attention in the sintering process control. Therefore, trying to increase the remnant polarization P_r may be a more practical choice.

For a single ferroelectric crystal with a single-domain, the remnant polarization P_r is a constant value determined by the crystal structure. However, for non-textured piezoelectric ceramics with randomly oriented crystallites (grains), which are separated by grain boundaries, the macroscopic P_r is influenced significantly by the poling process. It is known that poling is an important process to endow ferroelectric polycrystals with macroscopic piezoelectric responses, by applying a high electric field of up to several thousand volts per millimeter.[18] Inferior ferroelectric responses are obtained by insufficient poling, which is caused by various factors, such as defects. These defects can form an internal field that provides a driving force to switch the aligned domains back to their initial randomly distributed states.[19] On the other hand, it is well recognized that "A" site vacancies (V_A') (whereas oxygen vacancies $V_O^{\cdot\cdot}$ appear to neutralize the electric charge) are inevitable in KNN-based materials because of the high volatility of the alkaline elements (Li, Na, and K),[20] therefore, it is almost certain that simple poling of KNN-based ceramics is not satisfactory in most cases.

Nevertheless, defects can be exploited to benefit the electromechanical response in piezoelectrics. Recent studies have demonstrated that the utilization of point defects can lead to large recoverable electrostrains in acceptor-doped $BaTiO_3$ single crystals[21] as well as in ceramics,[22] and $KNbO_3$-based ceramics,[23] which is related to the symmetry-conforming migration of oxygen vacancies ($V_O^{\cdot\cdot}$). Besides $V_O^{\cdot\cdot}$, defect dipoles (D) that are composed of $V_O^{\cdot\cdot}$ and negatively charged defects, such as cation vacancies, can interact with spontaneous polarization (P_s) inside each domain, and result in giant electric-field-induced strains in $(Bi_{0.5}Na_{0.5})TiO_3$-$(Bi_{0.5}K_{0.5})TiO_3$-$BaTiO_3$ single crystals.[24]

In this paper, we demonstrate a new approach to further enhance the ferroelectric and piezoelectric properties of Li-doped KNN ceramics by manipulating the distribution of vacancy defects. The d_{33} constant can be significantly raised from 190 to 324 pC N^{-1}. In general, the polarization improvement was facilitated by domain engineering, which was implemented in practice by a re-poling process after room-temperature aging. It should be noted that the considerably improved d_{33} in the present study was the intrinsic piezoelectric constant measured under a small force field, suggesting promising applications in areas where bias power sources are not indispensable.

2. Results and Analysis

2.1. Structure Analysis and Enhanced Performances

The present study started with a series of Li-doped KNN ceramics. The X-ray diffraction (XRD) analysis showed that all the resultant

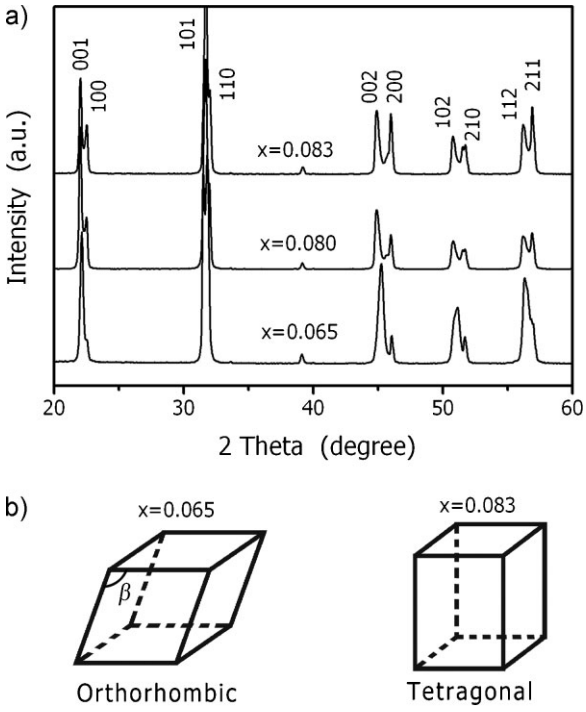

Figure 1. a) X-ray diffraction patterns of $(1-x)(Na_{0.535}K_{0.48})NbO_3$–$xLiNbO_3$ ($x = 0.065$, 0.080, 0.083) ceramics sintered at 950 °C. The peak indexing for a tetragonal perovskite phase was adopted. b) Illustration of orthorhombic and tetragonal perovskite primitive cell in an exaggerated manner.

materials have a perovskite structure, several of which are shown in Figure 1. The piezoelectric performance of KNN-based ceramics is especially sensitive to the perovskite phase structure, which is usually judged roughly by the relative intensities of the (002) and (200) peaks. For a typical orthorhombic phase (space group *Amm*2) with $x = 0.065$, the intensity of the (200) peak is more than twice that of the (002) one; while for a tetragonal phase (space group *P*4*mm*) with $x = 0.083$, the (002) peak is almost equal to the (200) one. It should be noted that the primitive cell of the orthorhombic perovskite structure is actually of monoclinic symmetry, as there is an angle β slightly larger than 90° (see Supporting Information). The Rietveld refinement of the powder X-ray diffraction data for $x = 0.080$ confirmed the two-phase coexistence situation, whereby the molar ratio of tetragonal to orthorhombic phase was roughly 7:3 (see Supporting Information). Therefore, it can be concluded that a phase transition occurs from the orthorhombic to the tetragonal phase with increasing $LiNbO_3$ amount; as a result, a two-phase coexistence region existed at room temperature from $x = 0.070$ to $x = 0.083$.

Figure 2a shows the piezoelectric coefficient d_{33} as well as the tetragonal–orthorhombic phase-transition temperature (T_{O-T}) of $LiNbO_3$–KNN ceramics as a function of $LiNbO_3$ content, after both the first and second poling, respectively. The T_{O-T} of the samples measured after the second poling was not perceptibly changed compared to that after the first poling. Even for sintering temperatures as low as 950 °C, a high piezoelectric constant d_{33} up to 280 pC N^{-1} was obtained at an optimal composition of $x = 0.083$ after the first poling. The basic mechanism for the

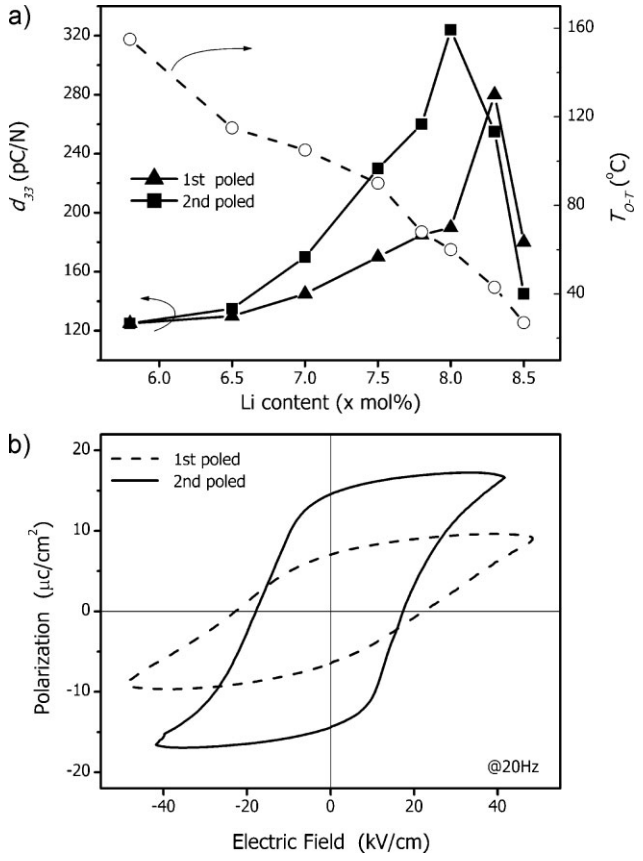

Figure 2. a) The piezoelectric coefficient d_{33} as well as the T_{O-T} of $(1-x)(Na_{0.535}K_{0.48})NbO_3$–$xLiNbO_3$ ceramics as a function of $LiNbO_3$ content, after both the first and second poling. b) Comparison of the *P*–*E* hysteresis loop for the sample with $x = 0.080$ after the first and second poling.

piezoelectric-property enhancement in the present study was generally considered to be related to the two-phase coexistence,[25] which can be seen by a decrease in T_{O-T} to around room temperature, as also shown in Figure 2. The listed T_{O-T} values, which were determined by dielectric constant anomalies as a function of temperature, were a little higher than the true phase-transition temperatures during heating-up cycles because of the thermal hysteresis effect. As a result, although the T_{O-T} for $x = 0.083$ was higher than 40 °C in Figure 2, the XRD results in Figure 1 revealed that the composition was much closer to a tetragonal phase than an orthorhombic one.

In spite of the considerably high piezoelectric performance of $LiNbO_3$-KNN ceramics after the first poling treatment, the improvement of d_{33} after the second poling process is much more attractive, with a maximum d_{33} of 324 pC N^{-1} at $x = 0.080$, as shown in Figure 2a. Such high d_{33} values have thus far only been obtained in $LiNbO_3$-KNN-based ceramics with codopants of Ta and Sb.[26,27] It should be noted that the increment in d_{33} after the second poling increased with increasing Li content, with a maximum increase of 134 pC N^{-1} (from 190 to 324 pC N^{-1}) at $x = 0.080$. The maximum increment was amazingly more than 70%, even though no special treatment was given to the samples apart from a re-poling after aging for two months. However, the sample with a d_{33} of 280 pCN^{-1} at $x = 0.083$ after the first poling showed no increase in d_{33} after re-poling two months later, on the contrary, its d_{33} decreased by 25 pC N^{-1}. It seems that aging and re-poling did not increase the d_{33} for samples with $x \geq 0.083$. In view of the T_{O-T} and XRD results, it could easily be concluded that samples with coexisting phases at room temperature are favorable for the aging and re-poling induced enhancement of piezoelectricity, while those dominated by orthorhombic (T_{O-T} more than 120 °C) or tetragonal phases are neither sensitive to the treatment nor profited from it. Figure 2b compares the *P*–*E* hysteresis loop for the sample with a Li amount of 8 mol % after the first and second poling. It was found that the second poling resulted in an increased P_r from 6.78 to 14.46 μC cm^{-2}, and a reduced E_c from 22.52 to 17.58 kV cm^{-1}. As indicated in Equation 1, the striking increase of d_{33} in the present study is related to the large improvement in P_r.

It was observed that the d_{33} coefficient measured after the first poling showed a slight decline with time whereas after the second poling it remained almost constant. For example, the sample with $x = 0.083$ showed a high d_{33} of 280 pC N^{-1} after the first poling, but the value decreased to 250 pC N^{-1} one month later. By contrast, the sample with $x = 0.080$, which achieved the highest d_{33} of 324 pC N^{-1} after the second poling, maintained a d_{33} of 320 pC N^{-1} after the same aging period. These results provide solid evidence that defect dipoles (*D*) can be located stably and compatibly with P_s after aging, so that their reverse-switching force after the second poling is negligible.

2.2. High-Angle X-ray Diffraction Observations and Domain Evolutions

As mentioned above, the increase of d_{33} in the present study was related to the large improvement in P_r, which was accomplished by domain switching. Domain switching does not change the crystalline structure of the ceramics, but it does have a striking influence on the macroscopic orientation of the local atom arrangement. XRD measurements can provide accurate information concerning these variations by the change in the relative peak intensity, wherefrom domain evolution processes can be deduced.[28]

Figure 3 shows the XRD patterns of the (222) and (004) lattice plane series for the $x = 0.065$, 0.080, and 0.083 samples, which were taken both before and after the first poling, as well as after the second poling. The peak indexing for an orthorhombic perovskite phase was adopted for the $x = 0.065$ sample, whereas that of a tetragonal phase was used for the $x = 0.080$ and 0.083 samples. High-angle X-ray diffraction offers more precise phase information than low-angle diffraction, which is usually employed in these types of studies.[29] For example, if the (222) diffraction forms a single peak, the sample has a tetragonal phase ($\beta = 90°$); whereas, if the (222) peak is obviously divided into two separate peaks, the sample is of orthorhombic structure ($90° < \beta < 91°$). Therefore, the obvious split of the (222) peak for the as-sintered sample shown in Figure 3a indicates a distinct orthorhombic phase structure. On the contrary, the sample shown in Figure 3c is much closer to a tetragonal phase, whereas the sample with $x = 0.080$ exhibits an intermediate XRD profile. As shown in Figure 3b, for the as-sintered sample, the higher intensity of the (400)/(040) peak over

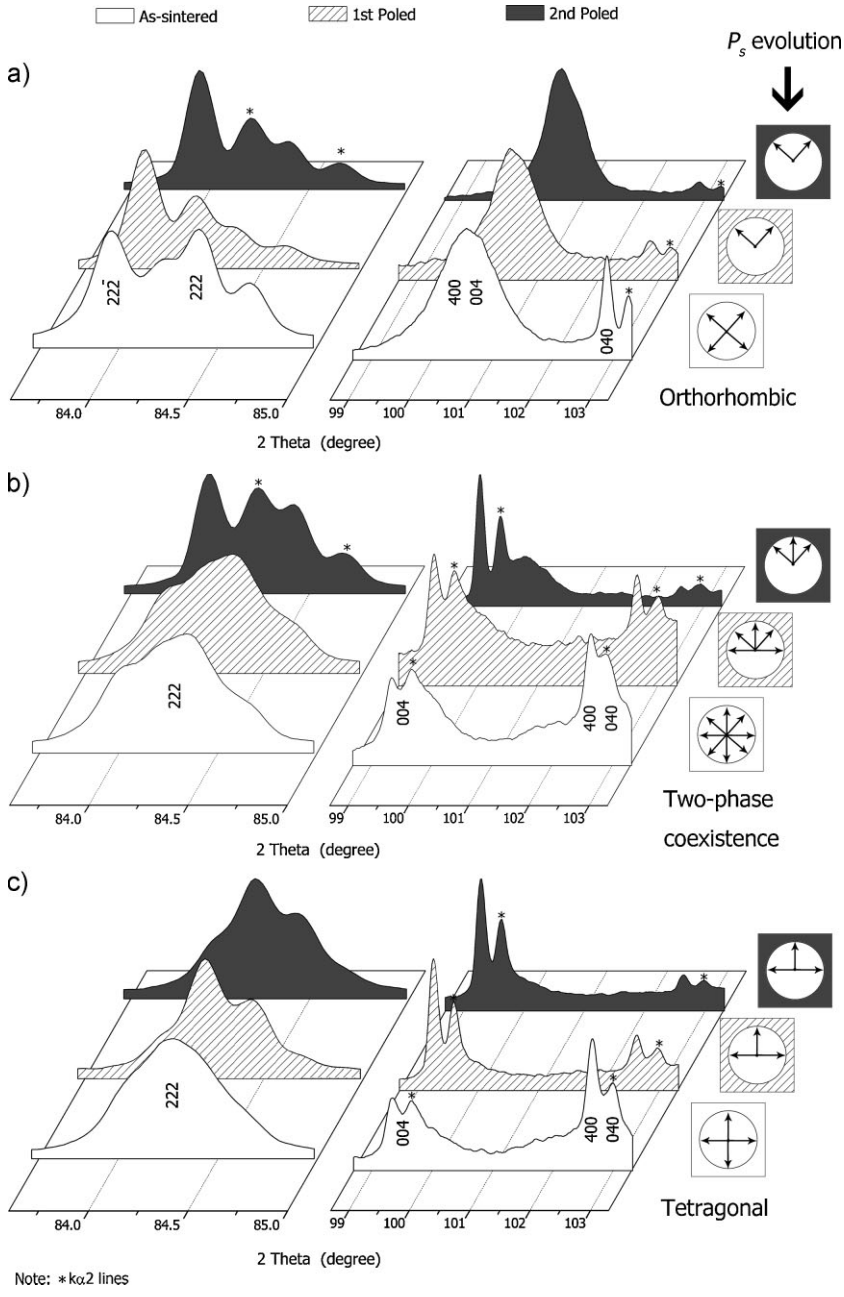

Figure 3. XRD patterns of the (222) and (004) lattice plane series for samples with a Li amount of a) 6.5 mol %, b) 8 mol %, and c) 8.3 mol %, both before and after the first poling, as well as after the second poling. The P_s evolution inside the domains is listed on the side, assuming that the electric field during the poling is parallel to the ⟨001⟩ direction.

the (004) peak is a clear sign of the tetragonal phase since $c > a = b$; however, the slight split of the (222) peak (see Supporting Information), and over-lifted kα2 line of the (004) peak indicate the presence of an orthorhombic phase ($a = c > b$ with $90^\circ < \beta < 91^\circ$). After the first poling treatment, the intensity contrast between the (400)/(040) peak and (004) peak reverses, which is easily understood for the tetragonal phase because of an increase in *c*-domains, as shown in Figure 3b,c. Intensity increments in the (004) peak after poling were also observed for the orthorhombic phase, despite the fact that ⟨001⟩ is not the spontaneous polarization direction, as shown in Figure 3a. The increased intensity of the (004) peak in the orthorhombic phase can be easily deduced as being a collateral consequence of the domain rotation towards the ⟨110⟩ direction, which will not be explained in detail here. It should be emphasized that, significant changes, represented by the distinct split of (222) peak and the near disappearance of the (400)/(040) peak, took place for the $x = 0.080$ sample after the second poling, as shown in Figure 3b. On the other hand, tiny variations in the XRD patterns were observed after the second poling for the other samples ($x = 0.065$ and 0.083) with no increase in d_{33}, as shown in Figure 3a,c.

The deduced P_s evolution inside the domains is listed on the side of Figure 3, assuming that the electric field during poling is parallel to the ⟨001⟩ direction. For the samples with evident orthorhombic ($x = 0.065$) or tetragonal ($x = 0.083$) phases (Fig. 3a,c), no obvious changes in P_s were found after the second poling, compared to that after the first poling. However, for the sample with the two-phase coexistence ($x = 0.080$) (Fig. 3b), the P_s parallel to the ⟨100⟩ and ⟨010⟩ directions after the first poling, switched to the ⟨001⟩ direction after the second poling, which indicates that the non-switched 90° domains were successfully rotated and kept in their place by means of the aging and re-poling process.

3. Discussion

To clarify the origin of aging and re-poling induced enhancement of piezoelectricity after re-poling in Li-modified KNN ceramics, a possible mechanism is proposed here. Figure 4a shows an ideal perovskite structure. However, because of inevitable volatilization of the alkali species in $LiNbO_3$-KNN, V_A' and $V_O^{\cdot\cdot}$ are formed during high-temperature sintering. In the present study, we measured the loss of alkali elements (Li, Na, and K) to be 1.3 mol % after sintering at 950 °C for 8 h in air, using inductively coupled plasma mass spectrometry (ICP-MS). A corresponding amount of V_A' should form in the ceramic samples after sintering, whereas $V_O^{\cdot\cdot}$ also appear to neutralize the electric charge. Since $LiNbO_3$-KNN has a cubic symmetry above the Curie temperature T_C, defects are distributed randomly, as shown in Figure 4b. After the first poling, 90° domains of tetragonal phases are maintained at a high level, which is proven by the existence of the (400)/(040) peak in Figure 3b. Affected by the macroscopic remnant polarization (P_r) after the first poling, defect dipoles (D), composed of V_A' and $V_O^{\cdot\cdot}$, gradually attain a stable configuration with a minimum-energy

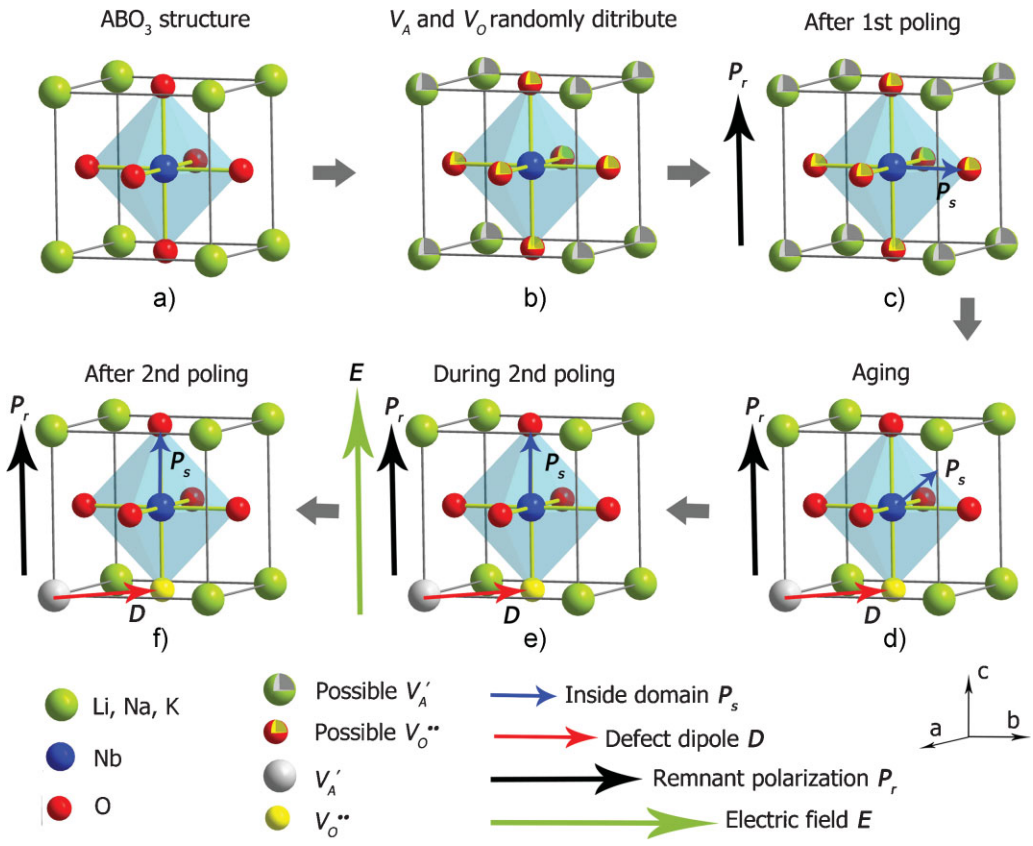

Figure 4. Schematic illustration for the aging-induced spontaneous polarization change in Li-modified KNN ceramics.

state perpendicular to P_r after aging, as shown in Figure 4d.[24] The new stable state cannot be attained immediately, since the exchange of ions is diffusive, which requires some time to accomplish (two months are sufficient for the present study). Although previous literature studies have shown the migration of $V_O^{\cdot\cdot}$ in solid solutions,[21–23] it is more likely that V_A' are actually more mobile than $V_O^{\cdot\cdot}$ in KNN-based materials, because of their smaller charge and size. In addition, D also influences the microscopic P_s inside the domains by short-range interactions, and the response of P_s is the crucial factor leading to changes in d_{33} after re-poling. The tetragonal and orthorhombic phases have similar energy states for samples with their composition close to $x = 0.080$, whereby the T_{O-T} is around room temperature, so P_s could rotate in the different modes of the two phases without too much difficulty.[4] For example, P_s turns from the ⟨010⟩ direction (spontaneous polarization direction in the tetragonal phase) in Figure 4c to the ⟨011⟩ direction (spontaneous polarization direction in the orthorhombic phase) in Figure 4d. During the second poling shown in Figure 4e, P_s easily rotates to become parallel to the electric field E (corresponding to a reduced E_c), and remains parallel after E was removed (corresponding to an increasing P_r), as long as the rotation in Figure 4d is achieved. The remaining of P_s (Fig. 4f) is also related to the similar energy states between both phases. In other words, the whole process could be summarized as an aging-assisted switching of the tetragonal 90° domains, which is strongly supported by the XRD results shown in Figure 3b. The polarization measurements shown in Figure 2b also offer solid evidence for this assumption, with an increasing P_r and decreased E_c for the same sample ($x = 0.080$) after the first and second poling, respectively.

Although the aging process could be accelerated at elevated temperatures,[23,30] for the present study it was carried out at room temperature, which is where the tetragonal–orthorhombic phase-transition temperature (T_{O-T}) takes place (for the sample with $x = 0.080$). The two-phase coexistence is the decisive factor for the occurrence of the subsequent rotation of P_s because of the equivalent energy states of the different domains belonging to distinct phases. The composition is another key factor. The aging-assisted switching of the 90° domains could not be achieved for samples with a T_{O-T} that was much higher or lower than room temperature, namely, the samples dominated by either the orthorhombic or tetragonal phase. The successful P_s rotation shown in Figure 4 requires equivalent energy states of the different domains belonging to distinct phases, which did not exist in the samples with $x = 0.065$ or $x = 0.083$. However, the phase transition from orthorhombic to tetragonal with Li content is a gradual process, and there is no straight line separating these two phases. As a result, for all samples with $0.065 \leq x \leq 0.083$, an improvement in d_{33} after the second poling is observed, however, the most obvious effect occurs for the sample with $x = 0.080$.

It should be pointed out that several other factors may contribute to the aging and re-poling induced enhancement of

piezoelectricity. In the present study, some samples were poled for as long as 4 h under a high voltage (6 kV cm^{-1}) during the first poling, however, no improvement in d_{33} was obtained. Thus, the poling conditions used in our experiments were sufficient. Moreover, the probability of an electric-field-induced phase transition during the second poling could also be excluded, since no perceptible change of either the T_{O-T} transition temperature or XRD peak position was observed. However, other factors such as strain relaxation or nanodomain wall migrations can not completely be ruled out.

4. Conclusions

Aging and re-poling induced enhancement of piezoelectricity in $(1-x)(Na_{0.535}K_{0.48})NbO_3$–$xLiNbO_3$ ($x = 0.058$–0.085) ceramics was investigated. A high d_{33} of 324 pC N^{-1} was obtained for the sample with $x = 0.080$, after a second poling treatment after the first poling and room-temperature aging for two months. A mechanism corresponding to details of spontaneous polarization change in the domain level was proposed, concerning the combined effect of the migration of oxygen vacancies, and interaction between defect dipoles and spontaneous polarization inside the domains. XRD and polarization measurements provided direct and strong evidence supporting our considerations. This discovery is a successful example of piezoelectricity enhancement in bulk ceramics by domain engineering, and will certainly be of great value for further exploration of high-performance lead-free piezoceramics.

5. Experimental

The ceramic samples, $(1-x)(Na_{0.535}K_{0.48})NbO_3$–$xLiNbO_3$ ($x = 0.058$–0.085), were prepared by a conventional ceramic processing route and sintering in air at a temperature as low as 950 °C. Commercial lithium carbonate (Li_2CO_3, 97.0%), sodium carbonate (Na_2CO_3, 99.8%), potassium carbonate (K_2CO_3, 99%), and niobium oxide (Nb_2O_5, 99.95%) were used as received. They were mixed according to a stoichiometric ratio with the nominal composition, followed by ball milling, with the aid of Y_2O_3-partially stabilized ZrO_2 ceramic balls, for 24 h in an ethanol solution. The mixed powders were calcined at 750 °C for 4 h and subjected to ball milling again for 24 h to enhance the compositional homogenization. The synthesized powders were then pressed into disks of 10 mm in diameter and 1 mm in thickness, followed by a cold-isostatic pressing under 200 MPa. Such pellets were sintered in air at 950 °C for 2 to 10 h. The bulk density of the sintered samples was measured by the Archimedes method. High-resolution X-ray diffraction (XRD) measurements using Cu Kα radiation (Rigaku, D/Max 2500) were carried out to determine the crystal phase. The Rietveld refinement was supported by the software Maud [31]. Inductively coupled plasma mass spectrometry (ICP-MS) was used to measure the loss of alkali elements during sintering. Samples were poled for the first time under a 3–6 kV mm^{-1} bias at 120 °C in a silicone oil bath for 30 min, and poled for the second time under the same conditions two months later. During the two months aging, the samples were kept under ambient condition without any special treatment. The piezoelectric properties were measured using a quasi-static piezoelectric constant testing meter (ZJ-3A, Institute of Acoustics, Chinese Academy of Science) after both the first and second poling, respectively. The dielectric constants were measured as a function of temperature in the range of −60 °C to 180 °C using an impedance analyzer (HP 4194A, Palo Alto, CA) to determine the orthorhombic–tetragonal phase-transition temperature (T_{O-T}). The polarization–electric field (P–E) hysteresis loops were measured using a ferroelectric tester (aixACC TF Analyzer 1000) at a fixed frequency of 20 Hz.

Acknowledgements

This work was supported by the National Nature Science Foundation of China (Grant Nos. 50772050 and 50921061) and the Ministry of Science and Technology of China under the Grant 2009CB623304, as well as by the Tsinghua University Initiative Scientific Research Program. Supporting Information is available online from Wiley InterScience or from the author.

Received: February 11, 2010
Published online: May 20, 2010

[1] E. Cross, *Nature* **2004**, *432*, 24.
[2] H. X. Yan, H. T. Zhang, R. Ubic, M. J. Reece, J. Liu, Z. J. Shen, Z. Zhang, *Adv. Mater.* **2005**, *17*, 1261.
[3] Y. Saito, H. Takao, T. Tani, T. Nonoyama, K. Takatori, T. Homma, T. Nagaya, M. Nakamura, *Nature* **2004**, *432*, 84.
[4] J. Rödel, W. Jo, K. T. P. Seifert, E. M. Anton, T. Granzow, D. Damjanovic, *J. Am. Ceram. Soc.* **2009**, *92*, 1153.
[5] S. J. Zhang, R. Xia, T. R. Shrout, *J. Electroceram.* **2007**, *19*, 251.
[6] Y. P. Guo, K. Kakimoto, H. Ohsato, *Appl. Phys. Lett.* **2004**, *85*, 4121.
[7] E. Hollenstein, M. Davis, D. Damjanovic, N. Setter, *Appl. Phys. Lett.* **2005**, *87*, 182 905.
[8] H. C. Song, K. H. Cho, H. Y. Park, C. W. Ahn, S. Nahm, K. Uchino, S. H. Park, *J. Am. Ceram. Soc.* **2007**, *90*, 1812.
[9] N. Klein, E. Hollenstein, D. Damjanovic, H. J. Trodahl, N. Setter, M. Kuball, *J. Appl. Phys.* **2007**, *102*, 014 112.
[10] D. Lin, K. W. Kwok, H. L. W. Chan, *J. Appl. Phys.* **2007**, *102*, 034 102.
[11] G. Z. Zang, J. F. Wang, H. C. Chen, W. B. Su, C. M. Wang, P. Qi, B. Q. Ming, J. Du, L. M. Zheng, S. J. Zhang, T. R. Shrout, *Appl. Phys. Lett.* **2006**, *88*, 212 908.
[12] H. L. Du, W. C. Zhou, F. Luo, D. M. Zhu, S. B. Qu, Z. B. Pei, *Appl. Phys. Lett.* **2007**, *91*, 202 907.
[13] K. Wang, J.-F. Li, N. Liu, *Appl. Phys. Lett.* **2008**, *93*, 092 904.
[14] P. Zhao, B. P. Zhang, J.-F. Li, *Appl. Phys. Lett.* **2007**, *90*, 242 909.
[15] D. Damjanovic, *J. Am. Ceram. Soc.* **2005**, *88*, 2663.
[16] A. Safari, E. K. Akdoğan, *Piezoelectric and Acoustic Materials for Transducer Applications*, Springer, New York, NJ **2008**, p. 21.
[17] G. Arlt, D. Hennings, G. Dewith, *J. Appl. Phys.* **1985**, *58*, 1619.
[18] H. Thomann, *Adv. Mater.* **1990**, *2*, 458.
[19] D. Damjanovic, *Rep. Prog. Phys.* **1998**, *61*, 1267.
[20] Y. H. Zhen, J.-F. Li, *J. Am. Ceram. Soc.* **2007**, *90*, 3496.
[21] X. B. Ren, *Nat. Mater.* **2004**, *3*, 91.
[22] L. X. Zhang, W. Chen, X. B. Ren, *Appl. Phys. Lett.* **2004**, *85*, 5658.
[23] Z. Y. Feng, X. B. Ren, *Appl. Phys. Lett.* **2007**, *91*, 032 904.
[24] S. Teranishi, M. Suzuki, Y. Noguchi, M. Miyayama, C. Moriyoshi, Y. Kuroiwa, K. Tawa, S. Mori, *Appl. Phys. Lett.* **2008**, *92*, 182 905.
[25] Y. J. Dai, X. W. Zhang, G. Y. Zhou, *Appl. Phys. Lett.* **2007**, *90*, 262 903.
[26] E. K. Akdoğan, K. Kerman, M. Abazari, A. Safari, *Appl. Phys. Lett.* **2008**, *92*, 112 908.
[27] R. Z. Zuo, J. Fu, D. Y. Lv, *J. Am. Ceram. Soc.* **2009**, *92*, 283.
[28] S. Li, A. S. Bhalla, R. E. Newnham, L. E. Cross, *J. Mater. Sci.* **1994**, *29*, 1290.
[29] K. Wang, J.-F. Li, *Appl. Phys. Lett.* **2007**, *91*, 262 902.
[30] W. F. Liu, W. Chen, L. Yang, L. X. Zhang, Y. Wang, C. Zhou, S. T. Li, X. B. Ren, *Appl. Phys. Lett.* **2006**, *89*, 172 908.
[31] Details concerning Maud can be found at http://www.ing.unitn.it/~Maud/index.html (accessed December 2009).